Applied Physics Letters

RESEARCH ARTICLE | MARCH 12 2025

Low energy backgrounds and excess noise in a two-channel low-threshold calorimeter

R. Anthony-Petersen ; C. L. Chang ; Y.-Y. Chang ; L. Chaplinsky ; C. W. Fink ; M. Garcia-Sciveres ; W. Guo ; S. A. Hertel ; X. Li ; J. Lin ; M. Lisovenko ; R. Mahapatra ; W. Matava; D. N. McKinsey; D. Z. Osterman ; P. K. Patel ; B. Penning ; M. Platt; M. Pyle ; Y. Qi ; M. Reed ; I. Rydstrom ; R. K. Romani ; B. Sadoulet; B. Serfass ; P. Sorensen ; B. Suerfu ; V. Velan ; G. Wang ; Y. Wang ; S. L. Watkins ; M. R. Williams

Appl. Phys. Lett. 126, 102601 (2025)
https://doi.org/10.1063/5.0247343

Applied Physics Letters ARTICLE pubs.aip.org/aip/apl

Low energy backgrounds and excess noise in a two-channel low-threshold calorimeter

Cite as: Appl. Phys. Lett. **126**, 102601 (2025); doi: 10.1063/5.0247343
Submitted: 6 November 2024 · Accepted: 28 February 2025 ·
Published Online: 12 March 2025

R. Anthony-Petersen,[1] C. L. Chang,[2,3,4] Y.-Y. Chang,[1] L. Chaplinsky,[5] C. W. Fink,[1,6] M. Garcia-Sciveres,[7,8] W. Guo,[9,10] S. A. Hertel,[5] X. Li,[7] J. Lin,[1,7] M. Lisovenko,[2] R. Mahapatra,[11] W. Matava,[1] D. N. McKinsey,[1,7] D. Z. Osterman,[5] P. K. Patel,[5] B. Penning,[12] M. Platt,[11] M. Pyle,[1] Y. Qi,[9,10] M. Reed,[1] I. Rydstrom,[1] R. K. Romani,[1,a)] B. Sadoulet,[1] B. Serfass,[1] P. Sorensen,[7] B. Suerfu,[8] V. Velan,[7] G. Wang,[2] Y. Wang,[1] S. L. Watkins,[1] and M. R. Williams[7]

AFFILIATIONS

[1]University of California Berkeley, Department of Physics, Berkeley, California 94720, USA
[2]Argonne National Laboratory, 9700 S Cass Ave, Lemont, Illinois 60439, USA
[3]Kavli Institute for Cosmological Physics, The University of Chicago, Chicago, Illinois 60637, USA
[4]Department of Astronomy and Astrophysics, The University of Chicago, Chicago, Illinois 60637, USA
[5]University of Massachusetts, Amherst Center for Fundamental Interactions and Department of Physics, Amherst, Massachusetts 01003-9337, USA
[6]Now at Los Alamos National Laboratory, Los Alamos, New Mexico 87545, USA
[7]Lawrence Berkeley National Laboratory, 1 Cyclotron Rd., Berkeley, California 94720, USA
[8]International Center for Quantum-field Measurement Systems for Studies of the Universe and Particles (QUP,WPI), High Energy Accelerator Research Organization (KEK), Oho 1-1, Tsukuba, Ibaraki 305-0801, Japan
[9]Department of Mechanical Engineering, FAMU-FSU College of Engineering, Florida State University, Tallahassee, Florida 32310, USA
[10]National High Magnetic Field Laboratory, Tallahassee, Florida 32310, USA
[11]Texas A&M University, Department of Physics and Astronomy, College Station, Texas 77843-4242, USA
[12]University of Zurich, Department of Physics, 8057 Zurich, Switzerland

[a)]**Author to whom correspondence should be addressed:** rkromani@berkeley.edu

ABSTRACT

We describe observations of low energy excess (LEE) events, background events observed in all light dark matter direct detection calorimeters, and noise in a transition edge sensor based two-channel silicon athermal phonon detector with 375 meV baseline energy resolution. We measure two distinct LEE populations: "shared" multichannel events with a pulse shape consistent with substrate athermal phonon events and sub-eV events that couple nearly exclusively to a single channel with a significantly faster pulse shape. These "singles" are consistent with events occurring within the aluminum athermal phonon collection fins. Similarly, our measured detector noise is higher than the theoretical expectation. Measured noise can be split into an uncorrelated component, consistent with shot noise from small energy depositions within the athermal phonon sensor itself, and a correlated component, consistent with shot noise from energy depositions within the silicon substrate's phonon system.

The search for dark matter (DM) has expanded to lower mass candidates, including sub-GeV "light mass" DM.[1–5] Direct detection of light mass DM scattering off nuclei, electrons, or crystal lattices requires extremely low energy thresholds, given the low kinetic energy carried by the DM particles. Cryogenic calorimeters are well suited to attaining such low thresholds and have recently set limits on sub-GeV DM-nucleon interaction cross sections.[6–8] These calorimeters typically read out athermal phonons from a crystalline substrate using transition edge sensors (TESs)[9] connected to aluminum athermal phonon collection fins (forming

structures known as quasiparticle-trap-assisted electrothermal-feedback TESs: QETs[10]).

Calorimetric DM direct detection experiments and other low threshold calorimeters have observed an excess of events below several hundred eV, with a rate that rises dramatically at low energies.[6,7,11] The rate of these low energy excess (LEE) events decreases with time, and can be regenerated by warming up the detector.[12] Additionally, the LEE rate varies only weakly with detector material or mass,[12] and appears similarly in detectors run above and below ground.[13]

The decrease in the LEE rate with time suggests a relaxation mediated process. Mechanical stress relaxation in the detector holding has been shown to create LEE-like events;[14,15] however, a LEE population remains even in detectors held in low stress configurations[15] (when not discriminating between "singles" and "shared" LEE, as we do here), implying that additional relaxation processes are necessary to explain observations.

Stress created by the thermal contraction of sensor films relative to thick detector substrates has been proposed as another LEE source.[15] This stress would be present in all calorimeters observing the LEE, largely independent of the detector material or size.

If relaxation within films is responsible for the LEE, we expect some partitioning of energy between local deposition in the film's electronic system and phonon energy that leaks into the substrate. For example, athermal phonon bursts within the aluminum QET should break Cooper pairs and locally deposit energy.[16,17] A detector instrumented with multiple individually read out athermal phonon sensors would measure this localized energy deposition and therefore be able to discriminate LEE events (with significant local energy absorption) from DM interactions in the bulk substrate (that approximately uniformly excite all phonon sensors). This detector architecture has previously been shown by CRESST[18] and contemporaneously by our group[19] to have great potential. Around this time, a version of the film relaxation model briefly proposed in Ref. 15 was more fully developed and published.[20] This model attempted to explain LEE phonon bursts through the relaxation of thermally stressed aluminum films on the device surface. During the early experimental work,[19] limited control of systematics and understanding of pulse shapes for locally absorbed events constrained our ability to draw strong conclusions about sources of LEE. These limitations have now been remedied.

To test this LEE discrimination concept, a 1 cm-square, 1 mm-thick silicon substrate was instrumented with two channels of 25 tungsten TESs (∼48 mK Tc, nominally 40 nm thick) connected to aluminum athermal phonon collection fins (QETs,[10] 600 nm thick), covering 1.38 % of the device's surface (see Fig. 1). QETs were electrically connected by partially overlapping their aluminum fins, such that each channel of 25 TESs was read out as one unit. Unfortunately, during manufacturing, a fraction of the TESs were partially etched away, leading to some performance degradation (higher normal resistance and worse phonon collection efficiency). See supplementary material section C and Fig. S4 for further discussion. While performance in both channels was still acceptable, we focus on the left channel, which was less negatively impacted. As in Ref. 15, this detector was suspended from wire bonds to minimize LEE-type backgrounds associated with detector holding. It was housed inside multiple layers of electromagnetic interference (EMI) and infrared (IR) shielding at the base stage of a dilution refrigerator, and was read out using DC SQUID array amplifiers.

The detector was calibrated with optical photons to characterize its response to events of a known energy (see Fig. 2). Pulses of photons from a 405 nm (3.061 eV) room temperature laser were transmitted to the device using a single mode optical fiber terminated with a diffuser, which dispersed photons across the entire instrumented side of the

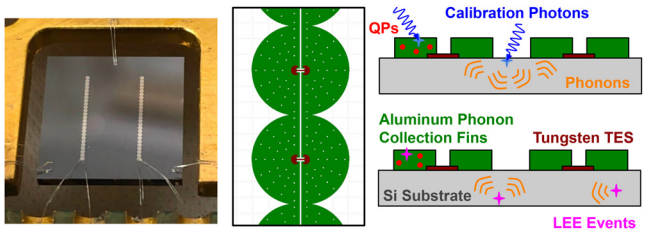

FIG. 1. (Left) Photograph of our 1 cm × 1 cm × 1 mm thick silicon athermal phonon detector. Two columns of QETs compose our phonon sensors, which are connected to a readout PCB (below) with wire bonds. The device is suspended by wire bonds as in Ref. 15 to suppress detector holding backgrounds. A gold wire bond (left) serves to cool the device. (Center) details of the QET[10] design, showing aluminum phonon collection fins (green), the tungsten/aluminum overlap region (purple half circle), and tungsten TESs (purple rectangles connecting overlap regions). For scale, the QET fins are 140 μm in radius. As the aluminum is deposited over the half-moon shaped W/Al overlap region, only the thin rectangular W TES is visible to calibration photons from above. 25 quasi-circular QETs are wired in parallel to form a channel. (Right Top) Sketch of the interaction of calibration photons with the detector, creating phonon (orange) or quasiparticle (QP, red) bursts in the detector substrate or aluminum QET fins, respectively. (Right Bottom) Sketch of LEE events, causing both phonon bursts in the detector substrate and quasiparticle bursts in the aluminum QET fins.

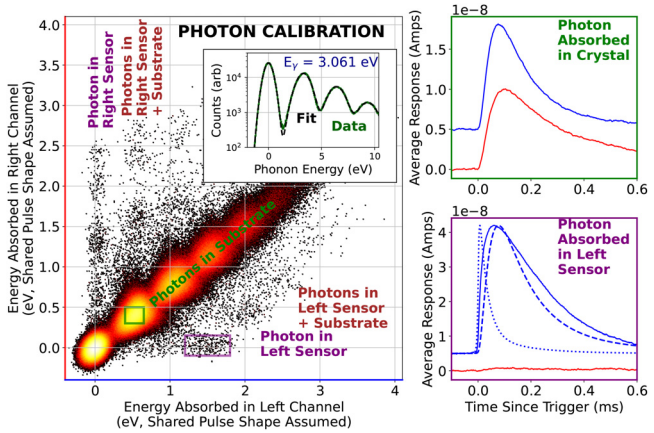

FIG. 2. (Left) Two-dimensional histogram of energy absorbed in the left (blue) and right (red) channels on the detector during photon calibration, assuming a phonon-like pulse shape. (Inset) Histogram of combined phonon energies (see supplementary material section C for further discussion of this combination technique), with multi-Gaussian fit (dashed). (Right) Average response for substrate (top; green box in the left panel) and direct hit (bottom; purple box in the left panel) events. Traces are filtered above 50 kHz and offset vertically for clarity. Solid red and blue correspond to the right and left channel responses, respectively. Dashed line shows the phonon template, while dotted line shows the modeled TES response to Dirac delta impulses. Note that energy reconstruction in this plot assumes a pulse shape for substrate/shared/phonon events, and direct hit events will not be reconstructed at the correct energy. See supplementary material section C for further discussion of our energy reconstruction.

detector. The photon pulses were fast ($\sim 1\,\mu$s) compared to the electrical ($\sim 10\,\mu$s) and electrothermal ($\sim 100\,\mu$s) response times of the TESs. On average, ~ 0.76 photons hit the detector per pulse. We recorded calibration data for 3.5 h, firing laser pulses at 100 Hz, ultimately recording 1.26×10^6 calibration events. Immediately following the calibration, 3 h of background data were acquired, interleaved with periods where the TESs were characterized using IV and dIdV measurements.[9,21]

Both datasets were recorded continuously and triggered offline. For the calibration dataset, we triggered on a recorded logic signal in coincidence with the laser pulses. In the background dataset, events were triggered on the sum of the two detector channels using an optimum filter energy estimator.[22] See supplementary material section A for further discussion of triggering.

Standard quality cuts were applied to the triggered data to ensure that the detector was operating stably, and to reject periods of high environmental noise or abnormal device performance. These cuts were designed for high passage of randomly triggered events (79.5%) and for similar passage of high energy events to minimize selection biases. See supplementary material section B for additional discussion. The height of each event was fit with an optimal filter assuming a calibrated phonon pulse shape (see below) and was converted into an energy by applying a factor derived from the channels responsivity $\partial P/\partial I(f)$[23] modeled from the measured complex impedance $\partial V/\partial I(f)$.[24,25] Using this method, we estimate the amount of energy each event deposits in a given TES channel for an assumed pulse shape (rather than into the detector phonon system as a whole). We use this as the primary quantity we plot in Figs. 2, 3, and 5 as a subclass of events we observe clearly do not couple through the detector phonon system ("singles," see below). See supplementary material section C for further discussion of energy reconstruction.

Due to the strong similarities in the classes of observed events, we discuss the calibration and background datasets together.

In the calibration and background datasets (see Figs. 2 and 3), "shared" events couple roughly equally to both channels (diagonal band, left panels). These events feature a relatively slowly rising pulse (see top right panels), which can be well modeled as the sum of two exponential phonon pulses convolved with the detector responsivity ($\partial P/\partial I(f)$). Calibration and background events are identically shaped.

We associate these events with bursts of athermal phonons from the substrate, which couple roughly equally to both channels. (Phonons couple somewhat more strongly to the left channel, i.e., have a higher "phonon collection efficiency." See supplementary material section C for further discussion.) In the background dataset at low energies, we associate these "shared events" with non-sensor film LEE relaxation sources due to the lack of significant localized energy absorption within the channel. At high energies (group of events above 5 eV in the left channel in Fig. 3), the saturated event rate is roughly consistent with the expected rate of high energy events from environmental radioactivity and cosmic rays. See supplementary material section D for additional discussion.

In the calibration, these events are caused by photons absorbed in the substrate, creating quantized (0, 1, 2, etc., photons absorbed) bursts of athermal phonons. We combine the response in both channels using inverse variance weighting,[23] constructing a phonon energy estimator, and plot a combined calibration histogram (see Fig. 2, inset, and material section C for more details on this energy reconstruction).

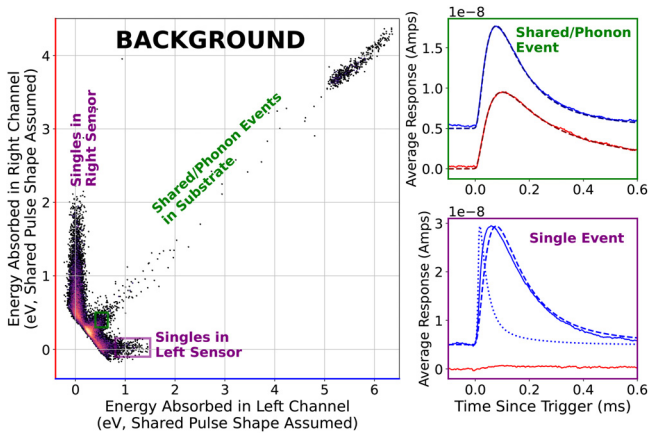

FIG. 3. (Left) Energies of background events in the left and right channels of the detector, assuming a phonon pulse shape and triggering on the sum of both channels. The group of events above 5 eV in the left channel are saturated events, consistent with cosmic rays and radiogenic backgrounds (see the supplementary material section D additional discussion). (Top right) shows the average responses for events in the green box (shared events) which match phonon templates derived from the photon calibration (dashed). (Bottom right) The averaged pulse shape for "single" events (purple box). Dashed line: phonon template and dotted line: modeled TES response to Dirac delta impulses. Traces are filtered above 50 kHz and offset vertically for clarity. Solid red and blue correspond to the right and left channel, responses. Note that energy reconstruction in this plot assumes a pulse shape for shared events, and singles will not be reconstructed at the correct energy. See supplementary material section C for further discussion of our energy reconstruction.

From this histogram, we measure a world leading baseline phonon energy resolution of $\sigma_P = 375.5 \pm 0.4$ meV (stat.), favorably comparing to previous detectors,[26,27] both with ~ 1 eV resolution.

Another class of events exhibits a nearly maximally asymmetric channel response (vertical and horizontal bands in Figs. 2 and 3), which we call "single" events due to their strong coupling to a single channel. In the calibration dataset, we attribute this response to events in which one photon hits an aluminum phonon collection fin, i.e., a "direct hit" event. Additional photons may be absorbed in the detector substrate, creating a superposition of "direct hit" and "substrate" events and forming the structure of black bands in Fig. 2. Of the roughly 4.1×10^5 single photon events seen in the substrate, we expect $\sim 1\,\%$ will hit a fin in a given channel, with $\sim 10\,\%$ of these photons being absorbed.[28] 239 events fall into the purple box in Fig. 2 (which contains roughly half of the left channel singles), in general agreement with the expected number of events. We attribute the spread in reconstructed energy to instrumental effects (e.g., position dependence within the aluminum and saturation from partial TESs etching), as well as the difference in the apparent distribution of singles energies (see supplementary material section C for further discussion). Given only 0.1 % of the QET area is exposed tungsten, we do not expect to observe a significant number of tungsten direct hits.

Pulse shapes for single events are shown in the bottom right panels of Figs. 2 and 3. The fast rise compared to substrate events (though somewhat slower than the modeled TES response to Dirac-delta energy impulses) indicates that the substrate phonon collection dynamics are bypassed. We attribute the slow fall of these events to saturation effects. Quasiparticles created by localized photon absorption

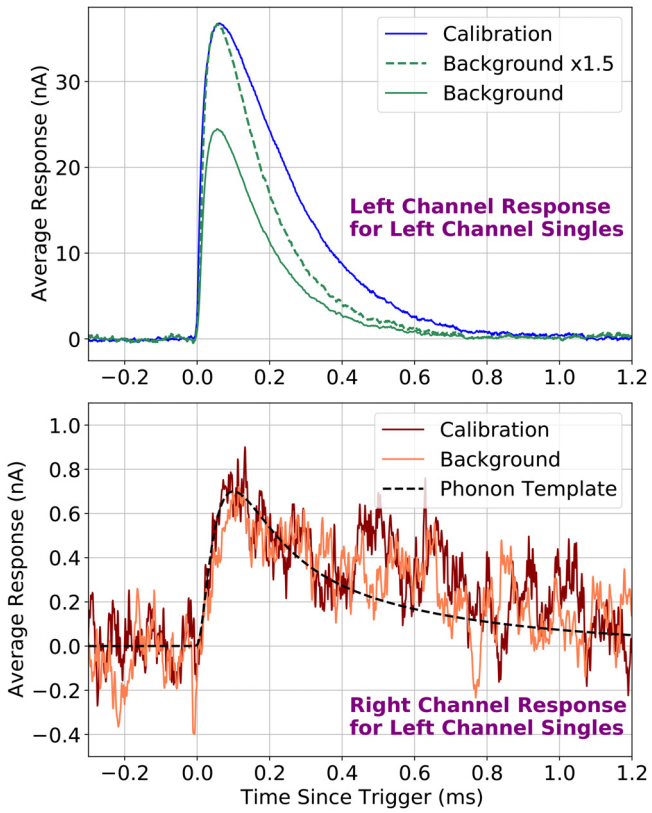

FIG. 4. Comparison between background and calibration left channel singles (purple boxed events in Figs. 2 and 3). Top shows the average main (left) channel response, while bottom shows the average right channel response when a single occurs in the left channel. The top dashed line is the rescaled background singles pulse, while the bottom dashed line is the calibrated response to athermal phonon pulses. For clarity, pulses are baseline subtracted and low pass filtered at 50 kHz.

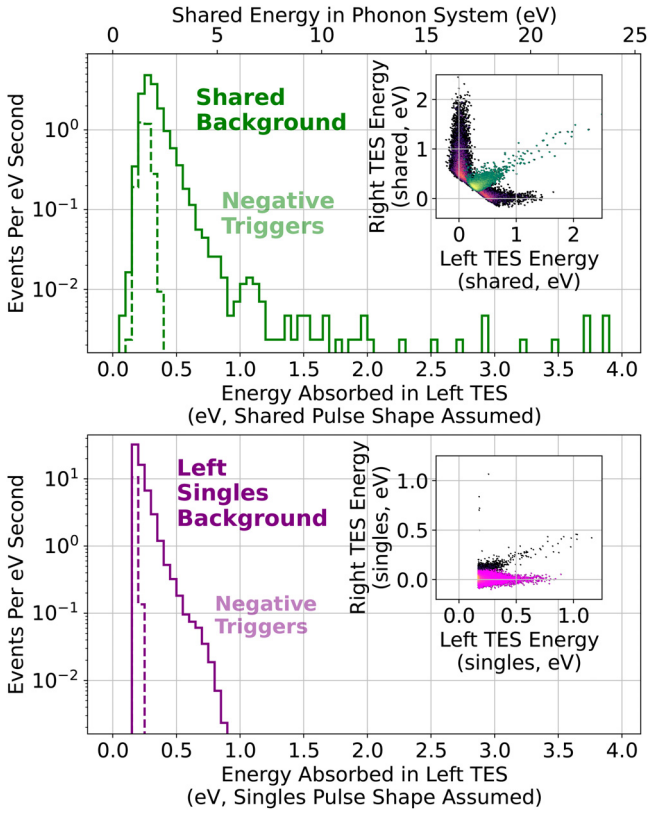

FIG. 5. Shared (green, top) and single (pink, bottom) backgrounds observed in the left channel of the detector. Dashed spectra (blue, purple) show negative amplitude events that sample noise trigger rates, demonstrating that LEE events are not predominantly noise fluctuations (see the text). Inset panels show events in left vs right energy space, with the single or shared events selected using a χ^2 based approach (see the text) highlighted in color. The top plots use shared energy estimators (the top inset plot is identical to Fig. 3, with shared events colored differently), and the bottom plots used singles energy estimators. See supplementary material sections A and C for more information on our triggering and energy reconstruction scheme.

would be expected to propagate to only a few of the 25 QETs in a channel, saturating these few TESs at energies significantly below the $\sim$5–6 eV of absorbed energy required to saturate all 25 QETs in a channel (see the group of saturated events at high energies in Fig. 3).

Comparing the pulse shapes of left singles in the background and calibration datasets (Fig. 4), we see broad qualitative consistency. After rescaling, the rising edge of the background and calibration singles pulses match, while the fall for (lower energy) background singles is faster than for calibration singles. This is expected from the saturation hypothesis: higher energy (calibration) singles would be expected to saturate more and therefore fall more slowly.

In the left singles events in Fig. 4, we see a small average response in the opposite (right) channel, carrying a few percent of the main channel's energy, in addition to the large average response in the primary (left) channel. The average opposite (right) channel responses for background and calibration events are indistinguishable and consistent with the calibrated athermal phonon response. We attribute this signal to athermal phonons that leak out of the aluminum fin during downconversion following a singles event. Notably, *without* rescaling the average background and calibration pulse shapes seen in the opposite (right) channel, these responses are roughly equal in height, suggesting that lower energy background events are more efficient in producing athermal phonons than calibration events and hinting that background singles may originate deeper within the aluminum fin.

In sum, we associate both calibration and background singles with events originating within an aluminum fin, locally saturating TESs close to the event and leaking out athermal phonons during the downconversion process. While calibration events are caused by photon absorption, background singles are caused by some unknown process that we broadly associate with LEE.

Bursts of high frequency (MHz-GHz) EMI[23] cannot be the primary source of these background singles, as individual EMI photons would not be sufficiently energetic to leak above the aluminum gap ($2\Delta_{Al} > (\sim 90\,\text{GHz}) \times h$) phonons into the substrate during the downconversion process. We also reject relaxation or other events occurring in the tungsten TESs as the source of background singles, as tungsten relaxation would be expected to produce a far larger pulse of athermal phonons in the substrate due to thinness of the tungsten film ($\sim$ 40 nm).[23]

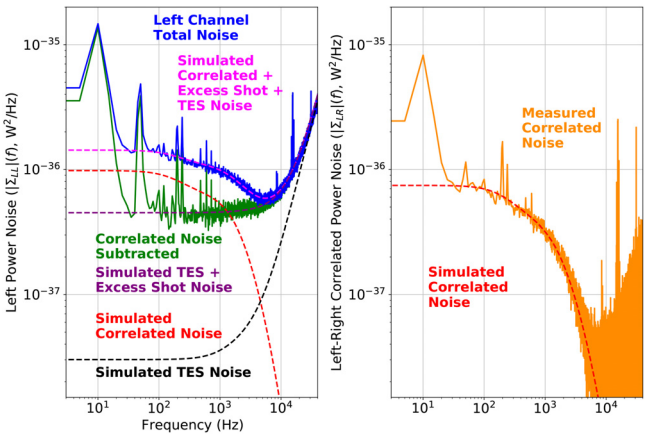

FIG. 6. (Left) Left channel total noise [blue, $|\Sigma_{LL}|(f)$], "uncorrelated" noise (green) after subtracting modeled correlated noise [red, dashed, $a\left|\frac{\partial P_R}{\partial E_p}\right|^2(f)$], modeled TES noise [black, dashed, $M_L(f)$], excess shot noise + modeled TES noise [purple, dashed, $M_L(f)+U_L$], and modeled noise including simulated excess correlated and shot terms (pink, dashed). (Right) Correlated noise [orange, $|\Sigma_{LR}|(f)$], fit to a phonon shot noise model [red, dashed, $a\left|\frac{\partial P_L}{\partial E_p}\frac{\partial P_R}{\partial E_p}\right|(f)$].

Photons incident on the QET fins (as in the calibration) would explain background singles. Above the silicon bandgap, these photons would also couple to the substrate, creating shared events. Future devices with improved resolutions should search for cutoffs in the shared spectrum at the silicon bandgap, characteristic of such photons.

Alternatively, the relaxation of thermally stressed aluminum films could create singles backgrounds. Romani[20] described a model where relaxing dislocations in an aluminum film impact the aluminum–substrate interface, injecting bursts of athermal phonons into the substrate while depositing minimal energy in the aluminum (i.e., forming shared events). Clearly, observed singles are in the opposite limit: they couple almost exclusively to the aluminum film. Modifying the model in Ref. 20 to include, e.g., damping of dislocations in the bulk film through the emission of above-gap phonons or phonon-emitting interactions with intra-film grain boundaries, might better explain singles events.

The background spectra for single and shared events are plotted in Fig. 5. Shared events were triggered on the sum of the two channels using a phonon template, while singles were triggered in the left channel using an averaged singles template. Since a given single or shared event could trigger both single and shared triggers, a χ^2 statistic considering the pulse shape and amplitude in both channels was used to discriminate event types and avoid double counting. If $\chi^2_{\text{single,left}} < (\chi^2_{\text{shared}}, \chi^2_{\text{single,right}})$, an event was classified as a left single, if $\chi^2_{\text{single,right}} < (\chi^2_{\text{shared}}, \chi^2_{\text{single,left}})$, it was a right single, and if $\chi^2_{\text{shared}} < (\chi^2_{\text{single,left}}, \chi^2_{\text{single,right}})$, it was determined to be a shared event. Inset plots in Fig. 5 show this χ^2 based on discrimination.

Above about 1 eV in the sensor ($\sim$6 eV in the phonon system), a slowly rising shared background dominates. At low energies, both singles and shared rates sharply and exponentially rise. While the similarities between spectra are at some level coincidental (plotting the shared channel in phonon units shows a different energy scale), we leave open the possibility that both low energy populations are caused by similar underlying processes.

To test whether the observed low energy excesses are noise artifacts, we invert the datastream and re-trigger, recording event-like noise fluctuations, which were previously negative. This samples the rate of random noise events. Positive amplitude (i.e., physical) events dominate over negative amplitude events (from noise, see the dashed spectra in Fig. 5), indicating that our backgrounds are predominantly true low energy events down to the trigger threshold.

TESs have relatively well understood noise performance, dominated by TES Johnson noise at high frequencies and thermal fluctuation noise (TFN) at frequencies below the primary dynamical pole of the TESs.[9] Noise in different TESs is expected to be uncorrelated.

In our detector, noise in both channels is significantly above the modeled noise and is correlated below several kHz (see Fig. 6). To elucidate the excess noise's source, we calculate the cross power spectral density (CSD) between the left and right channels for randomly triggered time periods, cutting periods with high noise or above-threshold events. We convert this current CSD into the power domain by applying a responsivity model $\partial P/\partial I(f)$ developed from the measured TES complex impedance $\partial V/\partial I(f)$.[21,24] The on-diagonal elements of the power CSD $|\Sigma|(f)$ measure the total noise in each channel, while the off diagonal elements of the CSD estimate the correlated noise.

As the measured correlated noise rolls off very close to the measured athermal phonon collection pole, we model the CSD as the sum of three terms: modeled TES noise $M_{L,R}(f)$, uncorrelated shot noise $U_{L,R}$, and phonon shot noise $a\left|\frac{\partial P_{L,R}}{\partial E_p}\frac{\partial P_{L,R}}{\partial E_p}\right|(f)$, where $\frac{\partial P_{L,R}}{\partial E_p}(f)$ are the measured responses of the channels to phonon events during the photon calibration,

$$|\Sigma|(f) = \begin{bmatrix} |\Sigma^2_{LL}(f)| & |\Sigma^2_{RL}(f)| \\ |\Sigma^2_{LR}(f)| & |\Sigma^2_{RR}(f)| \end{bmatrix} = \begin{bmatrix} M_L(f)+U_L+a\left|\frac{\partial P_L}{\partial E_p}\right|^2(f) & a\left|\frac{\partial P_R}{\partial E_p}\frac{\partial P_L}{\partial E_p}\right|(f) \\ a\left|\frac{\partial P_L}{\partial E_p}\frac{\partial P_R}{\partial E_p}\right|(f) & M_R(f)+U_R+a\left|\frac{\partial P_R}{\partial E_p}\right|^2(f) \end{bmatrix}. \quad (1)$$

Figure 6 compares this model to the measured noise, showing excellent agreement with only three degrees of freedom (a, U_L, U_R) and supporting the hypothesis that excess sub-threshold events create our observed excess noise. Sub-threshold LEE events that deposit energy instantaneously and locally within the sensor films would produce flat uncorrelated shot noise, while sub-threshold LEE events that generate a shared athermal phonon response would produce correlated shot noise with the observed frequency dependence.

Our observations are consistent with excess events (i.e., LEE) above and below threshold creating backgrounds and shot noise, respectively. With excess correlated noise and shared backgrounds, we observe phonon mediation and strong coupling to both channels. Similarly, we observe uncorrelated noise and singles that strongly couple to one channel and are inconsistent with substrate phonon events. If these excess noise terms are indeed LEE shot noise, LEE limits both resolution and backgrounds in our detector. Ultimately, mitigating this noise would allow us to achieve $\sim$60 meV sensitivities to phonon events, nearing the level needed to search for single optical phonons generated by dark matter interactions.[29]

Given the multiple classes of excesses, it seems plausible to attribute these events to multiple sources. For example, aluminum relaxation would naturally explain singles, while shot noise from GHz scale EMI bursts could dominate the uncorrelated noise. Likewise, different effects could dominate phonon backgrounds at different energy scales, e.g., high energy shared LEE might originate from the relaxation of radiation induced defects[30] or "microfractures"[14] within the substrate, while excess correlated noise could be caused by the absorption of, e.g., 40 meV photons emitted by the detector circuit board.[31] We leave disentangling these hypothesized contributions to future work studying excess rates and noise over time and their scaling with properties of the detector and surrounding materials.

In conclusion, we have demonstrated that two channel calorimeters provide key insights into excess noise and the LEE. Specifically, we show singles and uncorrelated noise are consistent with above and below threshold events in the aluminum sensor film. Additionally, these dual channel devices can be used to discriminate single LEE events that couple primarily to the sensor from events (and DM interactions) that couple to the detector phonon system, allowing for LEE to be partially discriminated in light DM searches. Understanding and disentangling these excesses will be key to unlocking meV-scale resolution phonon detectors and future highly motivated searches for light dark matter. Our results may also be of interest to the superconducting quantum device community, who have long observed excess quasiparticles in their aluminum devices.[32–34]

See the supplementary material for the details of our optimum filter based trigger scheme, our data quality cuts, the way in which we reconstruct the energy of triggered events, and the saturated events we see in our detector.

This work was supported in part by DOE (Grant Nos. DE-SC0019319, DE-SC0022354, and DE-SC0025523), and DOE Quantum Information Science Enabled Discovery (QuantISED) for High Energy Physics (No. KA2401032). This material is based upon the work supported by the National Science Foundation Graduate Research Fellowship (Grant No. DGE 1106400). This material is based upon the work supported by the Department of Energy National Nuclear Security Administration through the Nuclear Science and Security Consortium (Award Nos. DE-NA0003180 and/or DE-NA0000979). Work at Lawrence Berkeley National Laboratory was supported by the U.S. DOE, Office of High Energy Physics (Contract No. DEAC02-05CH11231). Work at Argonne is supported by the U.S. DOE, Office of High Energy Physics, (Contract No. DE-AC02-06CH11357). W.G. and Y.Q. acknowledge the support by the National High Magnetic Field Laboratory at Florida State University, which is supported by the National Science Foundation Cooperative Agreement (No. DMR-2128556) and the state of Florida.

AUTHOR DECLARATIONS

Conflict of Interest

The authors have no conflicts to disclose.

Author Contributions

R. Anthony-Petersen: Investigation (equal); Methodology (equal). **C. L. Chang:** Funding acquisition (equal); Writing – review & editing (equal). **Y. Y. Chang:** Investigation (equal); Methodology (equal); Writing – review & editing (equal). **L. Chaplinsky:** Writing – review & editing (equal). **C. W. Fink:** Investigation (equal); Methodology (equal); Software (equal); Writing – review & editing (equal). **M. Garcia-Sciveres:** Funding acquisition (equal); Writing – review & editing (equal). **W. Guo:** Funding acquisition (equal); Writing – review & editing (equal). **S. A. Hertel:** Funding acquisition (equal); Writing – review & editing (equal). **X. Li:** Software (supporting); Writing – review & editing (equal). **J. Lin:** Writing – review & editing (equal). **M. Lisovenko:** Writing – review & editing (equal). **R. Mahapatra:** Funding acquisition (equal); Investigation (equal); Writing – review & editing (equal). **W. Matava:** Writing – review & editing (equal). **D. N. McKinsey:** Funding acquisition (equal); Resources (equal); Writing – review & editing (equal). **D. Z. Osterman:** Writing – review & editing (equal). **P. K. Patel:** Software (supporting); Writing – review & editing (equal). **B. Penning:** Funding acquisition (equal); Writing – review & editing (equal). **M. Platt:** Investigation (equal); Methodology (equal); Resources (equal). **M. Pyle:** Conceptualization (equal); Formal analysis (equal); Funding acquisition (equal); Investigation (equal); Methodology (equal); Resources (equal); Supervision (equal); Validation (equal); Writing – original draft (equal); Writing – review & editing (equal). **Y. Qi:** Writing – review & editing (equal). **M. Reed:** Formal analysis (supporting); Investigation (equal); Methodology (equal); Software (equal); Writing – review & editing (equal). **I. Rydstrom:** Investigation (supporting); Methodology (supporting); Writing – review & editing (equal). **R. K. Romani:** Conceptualization (equal); Data curation (lead); Formal analysis (lead); Investigation (equal); Methodology (equal); Resources (equal); Software (equal); Validation (equal); Visualization (lead); Writing – original draft (lead); Writing – review & editing (lead). **B. Sadoulet:** Funding acquisition (equal); Supervision (equal); Writing – review & editing (equal). **B. Serfass:** Data curation (equal); Formal analysis (supporting); Investigation (equal); Methodology (equal); Resources (equal); Software (lead); Supervision (equal); Writing – review & editing (equal). **P. Sorensen:** Writing – review & editing (equal). **B. Suerfu:** Software (supporting); Writing – review & editing (equal). **V. Velan:** Writing – review & editing (equal). **G. Wang:** Methodology (supporting); Writing – review & editing (equal). **Y. Wang:** Writing – review & editing (equal). **S. L. Watkins:** Methodology (equal); Software (equal); Writing – review & editing (equal). **M. R. Williams:** Writing – review & editing (equal).

DATA AVAILABILITY

The data that support the findings of this study are available from the corresponding author upon reasonable request.

REFERENCES

[1]E. Kuflik, M. Perelstein, N. R.-L. Lorier, and Y.-D. Tsai, "Elastically decoupling dark matter," Phys. Rev. Lett. **116**, 221302 (2016).
[2]E. Kuflik, M. Perelstein, N. R.-L. Lorier, and Y.-D. Tsai, "Phenomenology of ELDER dark matter," J. High Energy Phys. **2017**, 78.
[3]Y. Hochberg, E. Kuflik, T. Volansky, and J. G. Wacker, "Mechanism for thermal relic dark matter of strongly interacting massive particles," Phys. Rev. Lett. **113**, 171301 (2014).
[4]Y. Hochberg, E. Kuflik, H. Murayama, T. Volansky, and J. G. Wacker, "Model for thermal relic dark matter of strongly interacting massive particles," Phys. Rev. Lett. **115**, 021301 (2015).

[5]L. J. Hall, K. Jedamzik, J. March-Russell, and S. M. West, "Freeze-in production of FIMP dark matter," J. High Energy Phys. **2010**, 80.
[6]A. Abdelhameed, G. Angloher, P. Bauer *et al.*, "First results from the CRESST-III low-mass dark matter program," Phys. Rev. D **100**, 102002 (2019).
[7]I. Alkhatib, D. Amaral, T. Aralis *et al.*, "Light dark matter search with a high-resolution athermal phonon detector operated above ground," Phys. Rev. Lett. **127**, 061801 (2021).
[8]G. Angloher, S. Banik, G. Benato *et al.*, "Results on sub-gev dark matter from a 10 eV threshold cresst-iii silicon detector," Phys. Rev. D **107**, 122003 (2023).
[9]K. Irwin and G. Hilton, "Transition-edge sensors," in *Cryogenic Particle Detection, Topics in Applied Physics*, edited by C. Enss (Springer, Berlin, Heidelberg, 2005), pp. 63–150.
[10]K. D. Irwin, S. W. Nam, B. Cabrera, B. Chugg, and B. A. Young, "A quasiparticle-trap-assisted transition-edge sensor for phonon-mediated particle detection," Rev. Sci. Instrum. **66**, 5322–5326 (1995).
[11]P. Adari, A. A. Aguilar-Arevalo, D. Amidei *et al.*, "EXCESS workshop: Descriptions of rising low-energy spectra," SciPost Phys. Proc. **9**, 001 (2022).
[12]G. Angloher, S. Banik, G. Benato *et al.*, "Latest observations on the low energy excess in CRESST-III," SciPost Phys. Proc. **12**, 013 (2023).
[13]M. Pyle, "Low energy event excess in calorimeters," public talk (2022); available at https://indico.scc.kit.edu/event/2575/contributions/9670/attachments/4814/7258/Pyle_EXCESS22.pdf.
[14]J. Astrom, P. Di Stefano, F. Probst *et al.*, "Fracture processes observed with a cryogenic detector," Phys. Lett. A **356**, 262–266 (2006).
[15]R. Anthony-Petersen, A. Biekert, R. Bunker *et al.*, "A stress-induced source of phonon bursts and quasiparticle poisoning," Nat. Commun. **15**, 6444 (2024).
[16]A. G. Kozorezov, A. F. Volkov, J. K. Wigmore *et al.*, "Quasiparticle-phonon downconversion in nonequilibrium superconductors," Phys. Rev. B **61**, 11807–11819 (2000).
[17]J. Martinis, "Saving superconducting quantum processors from decay and correlated errors generated by gamma and cosmic rays," npj Quantum Inf. **7**, 90 (2021).
[18]G. Angloher, S. Banik, G. Benato, A. Bento, A. Bertolini, R. Breier, C. Bucci, J. Burkhart, L. Canonica, A. D'Addabbo, S. Di Lorenzo, L. Einfalt, A. Erb, F. V. Feilitzsch, S. Fichtinger, D. Fuchs, A. Garai, V. M. Ghete, P. Gorla, P. V. Guillaumon, S. Gupta, D. Hauff, M. Ješkovský, J. Jochum, M. Kaznacheeva, A. Kinast, H. Kluck, H. Kraus, S. Kuckuk, A. Langenkämper, M. Mancuso, L. Marini, B. Mauri, L. Meyer, V. Mokina, M. Olmi, T. Ortmann, C. Pagliarone, L. Pattavina, F. Petricca, W. Potzel, P. Povinec, F. Pröbst, F. Pucci, F. Reindl, J. Rothe, K. Schäffner, J. Schieck, S. Schönert, C. Schwertner, M. Stahlberg, L. Stodolsky, C. Strandhagen, R. Strauss, I. Usherov, F. Wagner, V. Wagner, and V. Zema, "Doubletes detectors to investigate the cresst low energy background: Results from above-ground prototypes," Eur. Phys. J. C **84**, 1001 (2024).
[19]R. K. Romani, "Correlated and uncorrelated backgrounds and noise sources in athermal phonon detectors and other low temperature devices," in *20th International Conference on Low Temperature Detectors* (Cryogenics Society of Europe, 2023).
[20]R. K. Romani, "Aluminum relaxation as the source of excess low energy events in low threshold calorimeters," J. Appl. Phys. **136**, 124502 (2024).
[21]S. L. Watkins, "Athermal phonon sensors in searches for light dark matter," Ph.D. thesis (University of California, Berkeley, 2022).
[22]S. R. Golwala, "Exclusion limits on the WIMP-nucleon elastic-scattering cross section from the cryogenic dark matter search," Ph.D. thesis (University of California, Berkeley, 2000).
[23]R. K. Romani, Y.-Y. Chang, R. Mahapatra, M. Platt, M. Reed, I. Rydstrom, B. Sadoulet, B. Serfass, and M. Pyle, "A transition edge sensor operated in coincidence with a high sensitivity athermal phonon sensor for photon coupled rare event searches," Appl. Phys. Lett. **125**, 232601 (2024).
[24]M. A. Lindeman, B. Dirks, J. van der Kuur, P. A. J. de Korte, R. H. den Hartog, L. Gottardi, R. A. Hijmering, H. F. C. Hoevers, and P. Khosropanah, "Relationships between complex impedance, thermal response, and noise in tes calorimeters and bolometers," IEEE Trans. Appl. Supercond. **21**, 254–257 (2011).
[25]C. W. Fink, S. L. Watkins, T. Aramaki *et al.*, "Characterizing TES power noise for future single optical-phonon and infrared-photon detectors," AIP Adv. **10**, 085221 (2020).
[26]G. Angloher, S. Banik, G. Benato, A. Bento, A. Bertolini, R. Breier, C. Bucci, J. Burkhart, L. Canonica, A. D'Addabbo, S. Di Lorenzo, L. Einfalt, A. Erb, F. Feilitzsch, S. Fichtinger, D. Fuchs, A. Garai, V. Ghete, P. Gorla, P. Guillaumon, S. Gupta, D. Hauff, M. Ješkovský, J. Jochum, M. Kaznacheeva, A. Kinast, H. Kluck, H. Kraus, S. Kuckuk, A. Langenkämper, M. Mancuso, L. Marini, B. Mauri, L. Meyer, V. Mokina, M. Olmi, T. Ortmann, C. Pagliarone, L. Pattavina, F. Petricca, W. Potzel, P. Povinec, F. Pröbst, F. Pucci, F. Reindl, J. Rothe, K. Schäffner, J. Schieck, S. Schönert, C. Schwertner, M. Stahlberg, L. Stodolsky, C. Strandhagen, R. Strauss, I. Usherov, F. Wagner, V. Wagner, and V. Zema, "First observation of single photons in a cresst detector and new dark matter exclusion limits," Phys. Rev. D **110**, 083038 (2024b).
[27]E. Michielin, "Hvev detectors down at cute," in *eXCESS 2024 Workshop* (Sapienza Universita di Roma, 2024); available at https://agenda.infn.it/event/39007/contributions/235283/attachments/123151/180493/HVeVatCUTE.pdf.
[28]R. Flaschmann, C. Schmid, L. Zugliani, S. Strohauer, F. Wietschorke, S. Grotowski, B. Jonas, M. Müller, M. Althammer, R. Gross, J. J. Finley, and K. Müller, "Optimizing the growth conditions of Al mirrors for superconducting nanowire single-photon detectors," Mater. Quantum Technol. **3**, 035002 (2023).
[29]S. Knapen, T. Lin, M. Pyle, and K. M. Zurek, "Detection of light dark matter with optical phonons in polar materials," Phys. Lett. B **785**, 386–390 (2018).
[30]K. Nordlund, F. Kong, F. Djurabekova, M. Heikinheimo, K. Tuominen, and N. Mirabolfathi, "Defect recombination origin of low energy excess in semiconductor detectors," in *eXCESS 2024 Workshop* (Sapienza Universita di Roma, 2024); available at https://agenda.infn.it/event/39007/contributions/235291/attachments/123166/180513/excess2024_nordlund_videos.pdf.
[31]P. Du, D. Egana-Ugrinovic, R. Essig, and M. Sholapurkar, "Sources of low-energy events in low-threshold dark-matter and neutrino detectors," Phys. Rev. X **12**, 011009 (2022).
[32]E. T. Mannila, P. Samuelsson, S. Simbierowicz, J. T. Peltonen, V. Vesterinen, L. Grönberg, J. Hassel, V. F. Maisi, and J. P. Pekola, "A superconductor free of quasiparticles for seconds," Nat. Phys. **18**, 145–148 (2022).
[33]K. Serniak, M. Hays, G. de Lange, S. Diamond, S. Shankar, L. Burkhart, L. Frunzio, M. Houzet, and M. Devoret, "Hot nonequilibrium quasiparticles in transmon qubits," Phys. Rev. Lett. **121**, 157701 (2018).
[34]K. Dodge, C. Larson, K. Okubo, E. Yelton, and B. Plourde, "Characterization of thermalization timescales in superconducting qubits using quasiparticle poisoning rates," in *American Physical Society Annual Meeting* (APS, 2024); available at https://meetings.aps.org/Meeting/MAR24/Session/M52.10.